Experimental and Modeling Study of NH_3/C_2H_4 Combustion

Olivier Mathieu[1], Matthew Abulail[1,] Claire M. Grégoire[1], Ayam Mousse-Rayaleh[2], Alejandra Palomino[2], Nabiha Chaumeix[2], Hamid Hashemi[3], Peter Glarborg[3], Eric L Petersen[1]
[1]J. Mike Walker '66 Department of Mechanical Engineering, Texas A&M University
College Station, TX, USA
[2]ICARE, CNRS-INSIS
45100 Orléans, France
[3]DTU Chemical Engineering, Technical University of Denmark
DK-2800 Lyngby, Denmark

1 Introduction

To mitigate global warming, ammonia (NH_3) is a prime candidate to replace hydrocarbon fuels for energy production [1]. To counterbalance the well-documented drawbacks associated with ammonia use as a fuel, such as a very slow burning velocity and narrow flammability limits [2,3], a dual-fuel configuration is often considered. For instance, ammonia/methane mixtures have been extensively studied [4-6], since methane can be produced from biomass fermentation and is also the main component of natural gas. While studies have attempted to characterize the interactions between CH_4 and NH_3 in detailed kinetics models (see [7] and references therein), much less attention has been devoted to the interactions between ammonia and the combustion intermediates of methane/natural gas. One of these intermediates is ethylene, C_2H_4, which is also an important combustion intermediate of all hydrocarbons. Ammonia/ethylene mixtures were studied in a few recent studies focusing on ignition delay times [8], laminar flame speeds [9], or species time histories in shock tubes such as NH_3 [8] or CO, CO_2, H_2O, NH_3, and NO [10]. The aim of the present study is to complement this limited dataset to validate a detailed kinetic model. In this paper, the combustion of a 1:1 C_2H_4/NH_3 mixture was studied experimentally by measuring CO concentration time histories in a shock tube and laminar burning velocities in a spherical, closed vessel. The pressure was maintained at (laminar flame speed) or near (shock tube) atmospheric pressure, and several equivalence ratios were investigated. Results were compared to predictions from detailed kinetics models from the literature, namely the models from Elbaz et al. [11], Li et al. [12], Zhang et al. [13], Arunthanayothin et al. [14], and Glaborg and coworkers [15,16].

2 Experimental setups

2.1. Shock Tube and CO Diagnostic

Correspondence to: olivier.mathieu@tamu.edu

CO time-history profiles were measured in the Aerospace Shock Tube (AST) at Texas A&M University using a laser absorption diagnostic. The shock-tube facility is made of stainless-steel and has the following dimensions: 7.62-cm inner diameter and 3.25 m long for the driver section and 16.2-cm inner diameter and is 7.88 m long for the driven section; with these two parts separated by a single polycarbonate diaphragm. The extrapolated velocity to the endwall, measured using 5 piezoelectric pressure transducers over the last two meters, was used to calculate the temperature (T_5) and pressure (P_5) behind the reflected shock wave with 1-D normal shock equations (±1% and ±0.8%, respectively). Low pressures of 10^{-8} atm or less were achieved prior to each test. Optical window ports are located at the same axial plan near the endwall to enable laser absorption measurements. For this study, a 50/50 NH_3/C_2H_4 mixture was studied near atmospheric pressure at three equivalence ratios (ϕ) of 0.34, 1.0, and 2.0 in 99% diluent (about 20% He, and 79% Ar, with the exact mixtures listed in Table 1, along with the experimental conditions). Note that He was added to expedite the vibrational relaxation [17] of CO. Lastly, C_2H_4 comes from Praxair with a purity of 99.995%, and all the other gases (NH_3, O_2, He, and Ar) were provided by Linde with 99.999% purity (99.995% for NH_3).

CO concentration time histories were recorded behind reflected shock waves using a quantum cascade laser producing light at 2059.91 cm^{-1} to monitor the P(20) line of the $1 \leftarrow 0$ band for CO. The maximum absorption strength of the P(20) line was verified prior to each experiment with a removable cell containing a low-pressure mixture of 10% CO in Ar. The laser beam was split into two components: the time-resolved incident intensity (I_0) and the time-resolved transmitted intensity (I_t) that passes through the reacting gases, both collected by detectors in a direct absorption optical arrangement. These intensities are processed in conjunction with the Beer-Lambert relation to obtain the CO concentrations, X_{CO}: $I_t/I_0 = \exp(-k_v P L X_{CO})$, where P is the partial pressure, L the path length (inner diameter of the driven section, 16.2 cm), and k_v the absorption coefficient ($atm^{-1}cm^{-1}$). This CO diagnostic has an estimated error of around 5.5% [18]. Note that a laser absorption diagnostic was also employed for NH_3 measurements in this study [19]. However, it was found that C_2H_4 interacts with the wavelength selected at the combustion temperatures investigated. This broadband interaction was negligible at room temperature and this NH_3 diagnostic was thus used to determine the initial ammonia concentration in gas phase, an important information since ammonia adsorbs on the surface of the vessel [19]. The ammonia concentrations measured have a worst-case accuracy of ± 6% over the concentration reported in Table 1, with most cases being well under this uncertainty.

Table 1: Mixture composition and experimental conditions for $NH_3/C_2H_4/O_2$ mixtures in He/Ar.

ϕ	$\%_{NH3}$	$\%_{C2H4}$	$\%_{O2}$	$\%_{He}$	$\%_{Ar}$	T_5 (K)	P_5 (atm)
0.34	0.07675	0.07675	0.8465	20.41	78.59	1178 - 1573	1.36 ± 0.04
1.0	0.1739	0.1739	0.6522	20.02	78.98	1266 – 1914	1.28 ± 0.11
2.0	0.2581	0.2581	0.4838	20.02	78.98	1336 – 1992	1.24 ± 0.14

2.2. Closed Vessel and Laminar Flame Speed Measurements

The laminar flame speeds were measured at ICARE CNRS Orléans in a spherical vessel with an inner diameter of 563 mm (93.43 L vol.). This vessel is capable of reaching a maximum pressure of 200 bar with an initial temperature of 573 K and is equipped with 4 quartz windows (200-mm optical diameter). Two tungsten electrodes, mounted in the horizontal plane, are linked to a high-voltage discharge to create the electric spark necessary to ignite the mixture. This electric spark is also used to trigger the recording equipment (camera and oscilloscopes). The initial temperature was fixed at 323 ± 0.5 K thanks to the regulation of a thermo-fluid heating system. After ignition, the flame is visualized using a Z-shape Schlieren apparatus. A white continuous lamp (300 W Xe Lot-Oriel lamp) is used to illuminate the flame via two lenses and two concave spherical mirrors. The schlieren images of the growing flame were recorded with a high-speed camera (PHANTOM V1611), with an acquisition rate of ranging between

25,000 and 9,000 frames per second depending on the flame speed range. A homemade imaging processing system is used to extract the flame radius and hence obtain the flame trajectory $r_{flame} = f(time)$. The laminar flame speed is extracted from the flame radius using the non-linear expression of the flame speed versus stretch rate. More details about this vessel and the procedure are available in [20].

3 Experimental Results

3.1. CO concentration time histories

The CO profiles obtained during this study are visible in Fig. 1 for (a) $\phi = 0.34$, (b) $\phi = 1.0$, and (c) $\phi = 2.0$. For the fuel-lean and stoichiometric conditions, the CO formation starts after a delay that is temperature dependent (the lower the temperature, the longer the delay) and then reaches a peak (when the timeframe of the experiments allows). After the peak, the CO mole fraction steadily declines towards zero at the fuel-lean condition. For the stoichiometric case, this decline is relatively rapid at first but then reaches a pseudo plateau, with a very slow decline. The declining part past the peak is due to the oxidation of CO into CO_2. While the stoichiometric case is relatively typical to what is observed for hydrocarbons [17], the fuel lean case exhibits a CO consumption that is higher than typically observed for hydrocarbons in similar conditions. For the fuel-rich case (c), the lack of oxygen in the mixture prevents the conversion of CO into CO_2 and a plateau is reached after the initial growth period of CO.

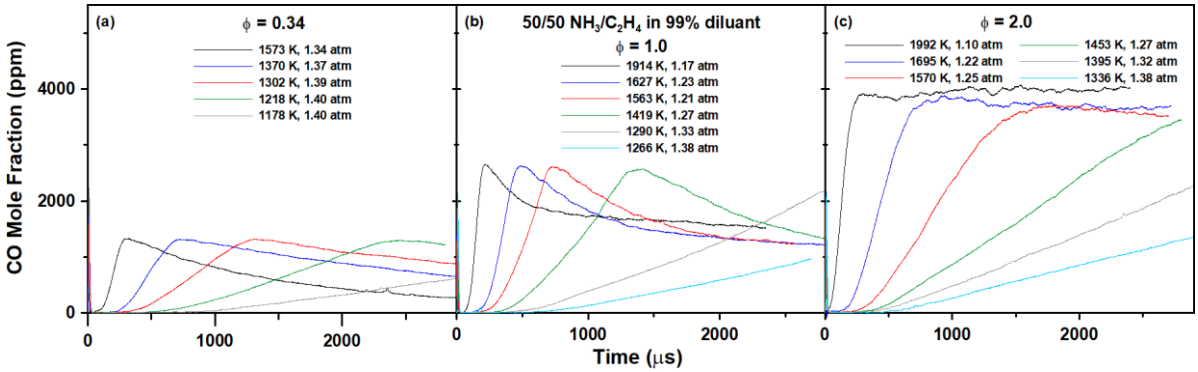

Figure 1: Evolution with time of the CO mole fractions during the oxidation 1:1 NH_3:C_2H_4 mixtures diluted in 99% Ar and He. (a) $\phi = 0.34$, (b) $\phi = 1.0$, and (c) $\phi = 2.0$.

3.2. Laminar Flame Speed

Figure 2 shows the evolution of the laminar flame speed at 1 atm and 323 K for mixtures of C_2H_4/air and 1:1 C_2H_4/NH_3 in air over a wide range of equivalence ratios ($\phi = 0.6$ - 2.0). Great care was taken in order to ensure that the laminar flame speed was not affected neither by the flame size nor by any deformation of its shape [20]. Since the recorded flames were up to a radius of 200 mm, the extracted laminar flame speed is independent for the method of derivation as it has been shown in our previous study [20]. The average standard error on the laminar flame speed is 0.5 cm/s. As can be seen, both mixtures exhibit the classical curve, with the maximum flame speed being recorded for slightly rich mixtures: around $\phi = 1.15$ for the neat C_2H_4 mixture, and near $\phi = 1.05$ for the mixture with ammonia. More importantly, when half of the fuel mixture consists of ammonia, the maximum laminar flame speed is reduced by more than 40%, from about 75.5 cm/s for the neat mixture to about 43.5 cm/s for the mixture with NH_3.

4 Model Comparison

Selected CO profiles from Fig. 1 are compared with the selected models from the literature in Fig. 3. For the fuel-lean case, (a), all models predict the shape well but are significantly under-reactive. The Glarborg and Elbaz models also slightly under-predict the amount of CO at the peak. On the other hand,

the stoichiometric case (b) is much better predicted overall, with the Glarborg one being the most accurate with regards to CO-peak timing. The Elbaz model is the closest to the data in terms of CO production at the peak, with the two Li and Zhang models being both over-reactive and over-predicting the CO mole fraction at the peak by more than 300 ppm, i.e. about 11%. The Arunthanayothin model also overpredicts CO by about 10% at the peak but is under-reactive. The Liu model is significantly under-reactive, and the least accurate, for all conditions investigated herein. Lastly, for the fuel-rich case (c), the Glarborg model is the most accurate for all criteria considered, with the Elbaz and Arunthanayothin models being strongly under-reactive and the two remaining ones being too reactive and over-predicting the CO mole fraction.

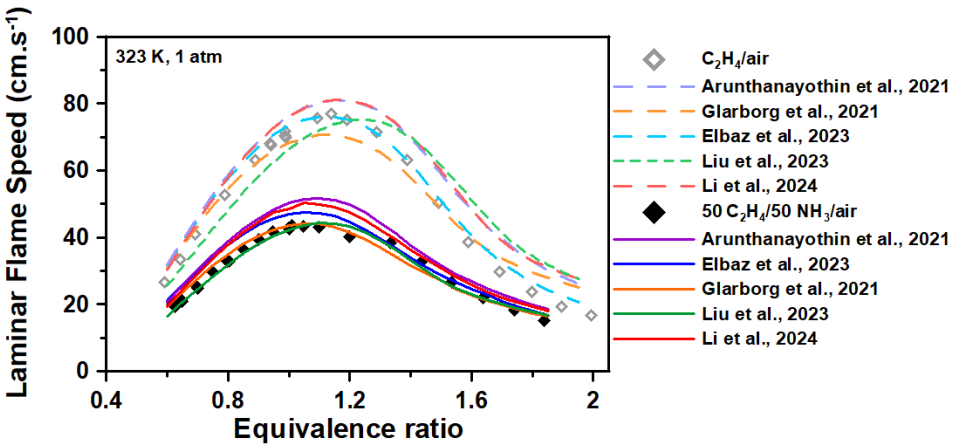

Figure 2: C_2H_4/air and 50 C_2H_4/50 NH_3 in air laminar flame speeds at 1atm and 323 K and comparison with detailed kinetics models from the literature.

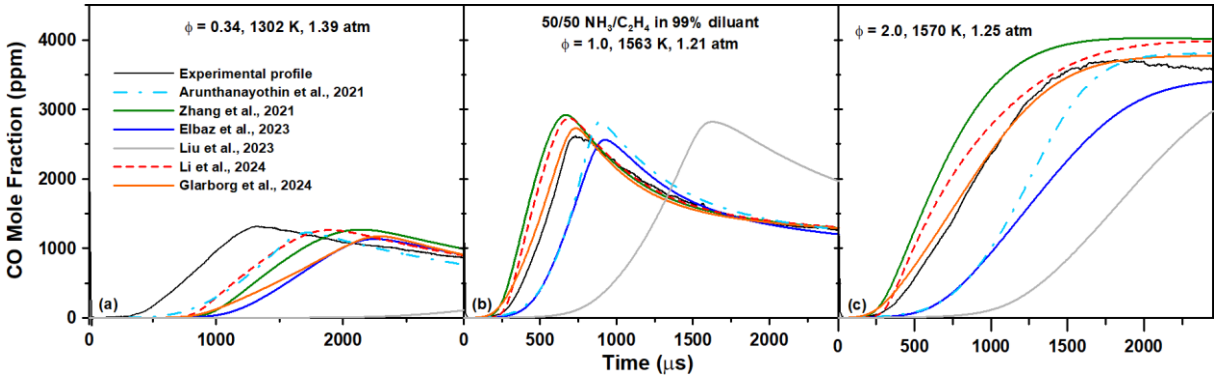

Figure 3: Evolution with time of selected CO mole fraction profiles during the oxidation 1:1 NH_3:C_2H_4 mixtures diluted in 99% Ar and He. (a) ϕ = 0.34, (b) ϕ = 1.0, and (c) ϕ = 2.0; and comparison with detailed kinetics models from literature.

For the laminar flame speed, the model comparison is visible in Fig. 2. Note that convergence issues were found for the Zhang model, even with its high-temperature version and using Chemkin or Cantera. For the neat C_2H_4 data, the Elbaz model accurately predicts the experimental results, whereas the Glarborg and Arunthanayothin models under- and over-predict it, respectively, by about 6-7%. Lastly, the maximum laminar flame speed is accurately predicted by the Liu model, but the curve is notably shifted toward the fuel-rich side. When 50% ammonia is present in the fuel mixture, the Glarborg model predicts the data with acceptable accuracy whereas the two other models over-predict the data: by about 10% at the maximum laminar flame speed for the Elbaz mechanism, and by about 20% for the Arunthanayothin mechanism. Like for the neat C_2H_4 mixtures, the shift toward the fuel-rich side is still

present when ammonia is added to the mixture for the Liu model, but the laminar lame speed is accurately predicted otherwise.

5 Conclusions

The interactions between ammonia and ethylene were characterized by experimentally measuring the laminar burning velocity and CO concentration time history of 1:1 NH_3/C_2H_4 mixtures over a range of equivalence ratios and at (laminar flame speed) or near (CO measurements) atmospheric pressure. The flame speed results showed that having 50% of ammonia in the fuel mixture reduces the maximum flame speed by about 40%, whereas the CO profiles were similar to those typically observed for neat hydrocarbons under similar conditions.

Models from literature were generally capable of predicting the overall trend of the data but room for improvement remains. For the CO concentration time histories, the fuel-lean mixture is poorly predicted by all models whereas the Glarborg model was relatively accurate for the other conditions investigated. The flame speed results showed that no model is capable of predicting both the data for the C_2H_4/air or C_2H_4/NH_3/air mixtures, showing that more work is required to characterize the interactions between ammonia and the double bound present in ethylene. Future work will focus on this area, and the resulting mechanism will serve as a foundation to better characterize the interactions between ammonia and hydrocarbons in dual-fuel systems.

6 Acknowledgments

The authors want to thank the financial support from the NSF under grant No. CBET-20308433 (Texas A&M University), CNRS-Ingénierie (ICARE-CNRS), and Innovation Fund Denmark (AFLOAT) (Technical University of Denmark).

References

[1] Mathieu O, Petersen EL. (2023). Carbon Free Fuels. ACS in Focus. American Chemical Society. (eISBN: 9780841299696).

[2] Valera-Medina A, Xiao H, Owen-Jones M, David WIF, Bowen PJ. (2018). Ammonia for power. Prog. Ener. Comb. Sci. 69: 63.

[3] Kobayashi H, Hayakawa A, Somarathne KDKA. (2019). Science and technology of ammonia combustion. Proceed. Comb. Inst. 37: 109-133.

[4] Okafor EC, Naito Y, Colson S, Ichikawa A, Kudo T, Hayakawa A, Kobayashi H. (2018). Experimental and numerical study of the laminar burning velocity of CH_4–NH_3–air premixed flames. Comb. Flame 187: 185.

[5] Zhang Z, Li A, Li Z, Ren F, Zhu L, Huang Z. (2024). An experimental and kinetic modelling study on the oxidation of NH_3, NH_3/H_2, NH_3/CH_4 in a variable pressure laminar flow reactor at engine-relevant conditions. Combust. Flame 265: 113513.

[6] Figueroa-Labastida M, Zheng L, Streicher JW, Hanson RK. (2024). High-temperature laminar flame speed measurements of ammonia/methane blends behind reflected shock waves. Combust. Flame 261: 113314.

[7] Guiberti TF, Pezzella G, Hayakawa A, Sarathy SM. (2024). Mini review of ammonia for power and propulsion: advances and perspectives. En. & Fuels 37: 14538.

[8] Shubao Song S, Jia W, Sun J, Wang C. (2024) Experimental and modeling study of the oxidation of NH_3/C_2H_4 mixtures in a shock tube. Combust. Flame 270: 113777.

[9] Liu B, Hu E, Yin G, Huang Z. (2023). Experimental and kinetic study on laminar burning velocities of ammonia/ethylene/air premixed flames under high temperature and elevated pressure. Combust. Flame 251: 112707.

[10] Zheng D, He D, Du Y, Li J, Zhang M, Ding Y, Peng Z. (2023). Experimental study of the methane/hydrogen/ammonia and ethylene/ammonia oxidation: Multi-parameter measurements using a shock tube combined with laser absorption spectroscopy. Combust. Flame 254: 112830.

[11] Elbaz AM, Giri BR, Shrestha KP, Arab OZ, Farooq A, Mauss F, Roberts WL. (2023). A comprehensive experimental and kinetic modeling study of laminar flame propagation of ammonia blended with propene. Combust. Flame 253: 112791.

[12] Li Y, Zhang Y, Fang J, Xi Z, Zhang J, Liu Z, Shi X, Li W. (2024). Combustion enhancement of ammonia by co-firing dimethyl ether/hydrogen mixtures under methane-equivalent calorific value. Combust. Flame 265: 113490.

[13] Zhang X, Yalamanchi KK, Sarathjy SM. (2023). Combustion chemistry of ammonia/C1 fuels: A comprehensive kinetic modeling study. Fuel 341: 127676.

[14] Arunthanayothin S, Stagni S, Song Y, Herbinet H, Faravelli T, Battin-Leclerc F. (2021). Ammonia–methane interaction in jet-stirred and flow reactors: An experimental and kinetic modeling study. Proceed. Comb. Inst. 38: 345.

[15] Glarborg P, Miller J.A, Ruscic B, Klippenstein SJ. (2018). Modeling Nitrogen Chemistry in Combustion, Prog. En. Combust. Sci. 67: 31-68.

[16] Jian J, Hashemi H, Wu H, Glarborg P, Jasper AW, Klippenstein SJ. (2024). An experimental, theoretical, and kinetic modeling study of post-flame oxidation of ammonia, Combust. Flame 261: 113325.

[17] Mathieu O, Mulvihill CR, Petersen EL. (2019). Assessment of modern detailed kinetics mechanisms to predict CO formation from methane combustion using shock-tube laser-absorption measurements. Fuel 236: 1164.

[18] Grégoire CM, Petersen EL, Mathieu O. (2023). Shock-tube CO measurements during the pyrolysis of ethylene carbonate. Combust. Flame 257: 113019.

[19] Alturaifi SA, Mathieu O, Petersen EL. (2022). An experimental and modeling study of ammonia pyrolysis. Combust. Flame 235: 111694.

[20] Hamadi A, Obrecht N, Callu C, Stagni A, Faravelli T, Comandini A, Chaumeix N. (2024). Experimental and modeling investigation of the laminar flame speeds for ammonia with various oxygen and diluent mixtures. Proceed. Comb. Inst. 40 (1-4), 105387.